Poly(lactic acid) composites reinforced with leaf fibers from ornamental variety of hybrid pineapple (Potyra)

Alfredo R. Sena Neto,[1] **Pedro I.C. Claro**,[2] **Fernanda V.D. Souza**,[3] **Luiz H.C. Mattoso**,[1] **José M. Marconcini**[1]

[1]*National Nanotechnology Laboratory for Agrobusiness (LNNA), Embrapa Instrumentation (CNPDIA), 13560-970 São Carlos, SP, Brazil*

[2]*PPGCEM/UFSCar, Washington Luiz Highway, 13565-905 Sao Carlos, SP, Brazil*

[3]*Embrapa Cassava and Tropical Fruits (CNPMF), 44380-000 Cruz das Almas, BA, Brazil*

While there have been many studies of fibers extracted from pineapple leaves as reinforcement in polymer composites, to date, only commercial varieties have been examined. This work aims to investigate the fibers from the leaves of a hybrid pineapple called Potyra as a mechanical reinforcement in a poly(lactic acid) (PLA) matrix. The fibers were pre-treated in a NaOH solution (1 wt%) and were incorporated into the PLA by a torque rheometer mixer followed by twin-screw extrusion. Samples of each composition were injected. The molded composites showed increases of tensile strength from 58.8 to 69.6 MPa, of Young's modulus from 1.9 to 3.5 GPa, and of impact resistance from 28 to 44 J/m, and showed an increase of 5°C in the heat deflection temperature (Abstract Figure). The measured tensile strength and Young's modulus values are lower than the theoretical values obtained by micromechanics theory due to the pull-out of the matrix fiber and due to the orientation of the fibers in the composites. It was concluded that the pineapple hybrid fibers have potential for use as mechanical reinforcement in green composites. POLYM. COMPOS., 00:000–000, 2017. © 2017 Society of Plastics Engineers

INTRODUCTION

Raw materials such as plant fibers and biodegradable polymers from renewable sources are an interesting alternative for the development of new materials with ecological appeal [1, 2].

Natural fibers have lower densities and are less expensive than synthetic fibers [3–5].

There are many studies of fibers obtained from commercial pineapple leaves (*Ananas comosus var. Comosus*) used as mechanical reinforcement in polymer composites [6–14], and the use of the curaua pineapple (*Ananas comosus var. erectifolius*) fibers as a mechanical reinforcement in composites is also already established [11]. Nevertheless, little is known about the possible use of leaf fibers derived from other genetic varieties of pineapple for mechanical reinforcement in composites [15].

Biodegradable polymers are advantageous relative to their non-biodegradable counterparts for easy disposal and pollution reduction [16]. Poly(lactic acid) (PLA) is a biodegradable polymer from renewable sources such as corn that is produced on a large scale and is marketed worldwide [17–21]. PLA has excellent strength and Young's modulus values compared to other biodegradable polymers, and even some synthetic polymers, which would justify its selection for use as the matrix in a composite. However, addition of vegetable fibers to the PLA matrix does not always result in an improvement of the mechanical properties [22–24].

In this work, the use of fibers extracted from the leaves of an ornamental variety of hybrid pineapple called Potyra as mechanical reinforcement in a PLA matrix was investigated.

MATERIALS AND METHODS

Materials

The following materials were used: PLA Ingeo 3251D with 1.24 g/cm^3 density and melt flow index of 35 g/10 min (190°C and 2.16 Kg) from Nature Works (Cargill®). Leaf fibers from a hybrid pineapple called Potyra from the Germplasm Bank of Embrapa Cassava and Tropical Fruits, Cruz das Almas-BA, Brazil. These fibers show Young's modulus of 73 GPa, tensile strength of 1,231 MPa, and initial degradation temperature of 264°C [25].

Correspondence to: A. R. Sena Neto; e-mail: alfredo.neto@deg.ufla.br
Contract grant sponsor: CAPES, CNPQ, PPGCEM/UFSCar, and Embrapa.
DOI 10.1002/pc.24464
Published online in Wiley Online Library (wileyonlinelibrary.com).

TABLE 1. Samples formulations, tensile strength, Young's modulus, elongation at break, HDT, notched Izod impact strength, onset temperatures (OOT), and crystallinity indexes for neat PLA and composites.

Samples	Potyra PALF (wt%)	Tensile strength (MPa)	Young's modulus (GPa)	Elongation at break (%)	HDT (°C)	Notched Izod impact (J/m)	OOT (°C)	%Xc
Neat PLA	—	58.8 (±1.5)	1.9 (±0.0)	3.3 (±0.2)	52.1 (±0.1)	28 (±3)	322	15%
Potyra 5%	5	54.5 (±0.3)	2.1 (±0.1)	3.2 (±0.1)	52.7 (±0.1)	26 (±1)	319	14%
Potyra 10%	10	56.6 (±0.3)	2.4 (±0.0)	3.1 (±0.0)	53.6 (±0.1)	27 (±2)	318	18%
Potyra 15%	15	59.5 (±0.4)	2.6 (±0.1)	3.0 (±0.1)	54.6 (±0.1)	32 (±1)	315	17%
Potyra 20%	20	63.4 (±0.2)	2.9 (±0.0)	3.0 (±0.1)	55.6 (±0.1)	37 (±2)	311	19%
Potyra 30%	30	68.2 (±1.1)	3.2 (±0.1)	3.0 (±0.1)	56.6 (±0.2)	42 (±2)	306	26%
Potyra 40%	40	69.6 (±1.5)	3.5 (±0.1)	2.8 (±0.2)	57.1 (±0.3)	44 (±4)	298	38%

Methodology

The Potyra (Potyra PALF) pineapple leaf fibers were ground in a mill with a grid mesh of 1.0 cm because fibers that are more than 1.0 cm long can lock equipment such as agitators, rheometers, and extruders. The fibers were then treated in a NaOH solution (1 wt%) at 70°C for 60 min under mechanical stirring. A pre-composite was produced in a torque rheometer (HAAKE Rheomix 600) under 50 rpm at 185°C for 2 min, with PLA to Potyra PALF (50 wt% of PLA and 50 wt% of pre-treated Potyra fiber) ratio of 1:1 (w/w). The pre-composite was added to the PLA pellets in a Baker and Perkins MP-19TC co-rotating twin-screw extruder under 95 rpm, with the following temperature profile of the feed channel to the matrix: 172°C, 170°C, 170°C, 175°C, and 180°C. Seven formulations were extruded: neat PLA; and composites with 5%, 10%, 15%, 20%, 30%, and 40% by weight of Potyra PALF (Table 1). The specimens were molded in an Arburg 270V automatic injector, using the temperature profile of the feed channel to the nozzle of 172, 170, 170, 175, and 180°C.

For each composition, five samples were subjected to a tensile test using an EMIC DL 3000 universal testing machine with the tensile speed of 5 mm.min^{-1} according to ASTM D638–10 and 10 samples were subjected to notched Izod impact using a Tinius Olsen equipment IT504, model following the ASTM D256 standard. Heat deflection temperature (HDT) was investigated for all compositions using a Vicat CEAST® equipment HDT 3 model with constant strength of 1.8 MPa applied in the middle of the specimen, heating rate of 2°C min^{-1}, and recording the temperature for the deflection of 0.25 mm, following ASTM D648–07. Thermogravimetric characterization was carried out using a Q500 TA Instruments® at the heating rate of 10°C min^{-1} under synthetic air atmosphere. Differential scanning calorimetry (DSC) was performed using Q100 TA Instruments equipment at temperatures between −20°C and 210°C at the heating rate of 10°C min^{-1}. The crystallinity indices were calculated according to:

$$\%X_C = \{[\Delta H_1 - (\Delta H_2 + \Delta H_3)]/(\Delta H_0)\} * 100 \quad (1)$$

where ΔH_1 is the enthalpy related to the melting peak (Tm); ΔH_2 and ΔH_3 are the enthalpies of the first and second crystallization peaks; and ΔH_0 is the enthalpy of fusion of a 100% crystalline PLA: 93.7 J/g [18]. For the morphological analysis, the injected sample were observed at cryogenic fracture using a scanning electron microscope JEOL JSM 6510 model with the electron acceleration voltage of 2.5–15 kV. The formulations were solubilized in dichloromethane and deposited on a slide, and their images were collected using a Leica DMRXP optical microscope with polarized light. The length and diameter of the fibers present in the formulations were estimated using the ImageJ program.

Micromechanics Theory

The theoretical calculation of the Young's modulus of fibers and fiber bundles was conducted using the Halpin–Tsai equation which includes the effects of the total fiber-matrix adhesion and assumes that defects are absent (*Eq. 2*). The Halpin–Tsai equation determines two Young's moduli according to the orientation of the fibers: the longitudinal Young's modulus (E_{cl}) for all fibers oriented in the load axis direction; and Young's modulus for all fibers oriented transverse to the load axis (E_{ct}). These modulus values help estimate the optimal Young's modulus for composites with randomly oriented fibers [26, 27]. The longitudinal Young's modulus (E_{cl}) and transverse Young's modulus (E_{ct}) may be obtained by:

$$E_c = \left(\frac{1+\xi\eta\phi_f}{1-\eta\phi_f}\right)E_m \quad (2)$$

where ϕ_f is the volume fraction of the fiber present in the composite (Table 4); E_m is the Young's modulus of the matrix; η is a relationship between the Young's modulus of the fiber (E_f) and matrix (E_m) (*Eq. 3*); and the ξ is the parameter related to the particle geometry and orientation of reinforcement relative to the axis of load application. For E_{cl} calculation, the ξ value is calculated as $2(l_f/d_f)$, where l_f is the fiber length and d_f is the fiber diameter. For E_{ct} calculation, ξ is equal to 2 [26, 27].

$$\eta = \frac{\left(\frac{E_f}{E_m} - 1\right)}{\left(\frac{E_f}{E_m} + \xi\right)} \quad (3)$$

The theoretical Young's modulus (E_{random}) for a composite with random fiber orientation can be calculated from E_{ct} and E_{cl} values as [26]:

DOI 10.1002/pc

$$E_{random} = \frac{3}{8}E_{cl} + \frac{5}{8}E_{ct} \quad (4)$$

The theoretical tensile strength value (σ_c) of a composite reinforced with short fibers can be determined by the "rule of mixtures" according to [26, 27]:

$$\sigma_c = \sigma_S \phi_f \left(1 - \frac{l_c}{2l_f}\right) k + \sigma'_m (1 - \phi_f) \quad (5)$$

where σ_s is the fiber tensile strength value (1,231 MPa for Potyra) [25]; σ'_m is the tensile strength measured on applying the deformation of 0.01916 mm*mm^{-1} in the pure matrix, corresponding to the elongation at break of Potyra fibers; and the factor k varies according to the short fibers' alignment, and is equal to 1/3 in this case (randomized alignment of the reinforcements on one plane). According to the study by Rosen [28], in the case of satisfactory fiber-matrix adhesion, fibers with the size above the minimum critical length (l_c) will show effective stress transfer from the matrix to the fibers and the mechanical strength of the composite will be greater than that of the pure matrix. The minimum critical fiber length (l_c) was determined as [28]:

$$l_c = \frac{d_f}{2}\left[\frac{\left(1 - \phi_f^{1/2}\right)}{\phi_f^{1/2}}\left(\frac{E_f}{G_m}\right)\right]^{1/2} .\cosh^{-1}\left[\frac{1 + (1-\phi)^2}{2(1-\phi)}\right] \quad (6)$$

where (ϕ) is the stress ratio; and G_m is the shear modulus of the matrix, calculated for an isotropic material by [26, 27]:

$$G_m = \frac{E_m}{2(1+\upsilon)} \quad (7)$$

where v is the Poisson ratio and E_m is the Young's modulus of neat PLA. The volume fraction (ϕ_f) was determined by *Eq. 8* (Table 4):

$$\phi_f = \frac{m_f/\rho_f}{\frac{m_f}{\rho_f} + \frac{(1-m_f)}{\rho_m}} \quad (8)$$

wherein the terms m_f and ρ_f are the fibers mass fraction and density, respectively; and ρ_m is the matrix density. The specific mass (obtained by pigmentary helium) was 1.510 g/cm^3 for treated Potyra PALF, and 1.260 g/cm^3 for PLA.

RESULTS AND DISCUSSIONS

Neat PLA shows the tensile strength value of 58.8 MPa and those of the composites ranged from 54.4 to 69.1 MPa. While the samples containing 5 and 10 wt% of Potyra PALF showed a slight reduction in tensile strength values with respect to the pure matrix, the tensile strength increased with increasing Potyra PALF mass fraction. The micrographs for composites containing 5 and 10 wt% of Potyra showed that these contained regions with higher and lower reinforcement concentrations. It is likely that this heterogeneity affects the tensile strength. The orientation, dispersion, and distribution of the fibers in lower amounts (5 and 10 wt%) in the polymer lead to the lower tensile strength relative to the tensile strength of neat PLA.

For the formulation with 40 wt%, the Potyra PALF average tensile strength value was 69.6 MPa, indicating that Potyra PALFs showed effective enhancement of mechanical characteristics. Araújo et al. [29] obtained PLA with curaua fibers composite without pre-treatment, observing a reduction in the tensile strength of up to 21% compared to neat PLA. They concluded that the pre-treatment of the fibers in their work was sufficient for improving the mechanical properties. PLA composite with cellulose extracted from newspapers received an increase of 8% in tensile strength compared to neat PLA [30]. PLA with 30% by weight of flax showed a 22% tensile strength increase and the tensile strength increased by 30% using 30% Cordenka by weight [31]. However, the resistance of these three latter materials did not reach 58 MPa.

The addition of Potyra PALF in PLA increased the Young's modulus, and demonstrated the direct relationship with the increasing PALF fraction. The pure matrix showed the Young's modulus value of 1.9 GPa, and the 40 wt% composite of Potyra PALF showed 3.5 GPa, an increase of 84% for this property (Table 1). These results are in agreement with other studies of the injection-molded PLA and lignocellulosic reinforcement, where the Young's modulus was increases by 56–103% [29–31].

The elongation at break ranged from $3.3 \pm 0.2\%$ for neat PLA to $2.8 \pm 0.2\%$ for the composite with 40 wt% of Potyra PALF (Table 1), which may be considered as an unaltered elongation at break, even with the increase in the tensile strength and Young's modulus.

There was an HDT increase of 5°C for composites with 40% PALF (Table 1). The PLA composite with 30 wt% of cellulose fibers extracted from newspaper increased the HDT by 16°C [30]. A PLA composite with 40 wt% wood fibers increased HDT by 3°C [32].

The impact strength values for Potyra 5% and Potyra 10% were reduced compared to the PLA matrix. Most likely, this arises from the orientation, dispersion and distribution of the fibers in lower amounts in the polymer, which is also the origin of the decreased tensile strength for the compositions with 5 and 10 wt% Potyra. For formulations with 15% or greater content by mass of Potyra PALF, there was an increase in the impact strength values relative to the value of neat PLA and the same behavior was observed for the tensile strength. The 40% Potyra formulation showed the impact strength value of 4.26 kJ/m^2, corresponding to the increase of 66% relative to the neat PLA (Table 1).

The PLA/curaua composites showed an impact strength gain by addition of 20 wt% of curaua to the composition [29]. A PLA composite with Cordenka also showed increased resistance to impact, unlike the PLA composites reinforced with flax that showed an impact

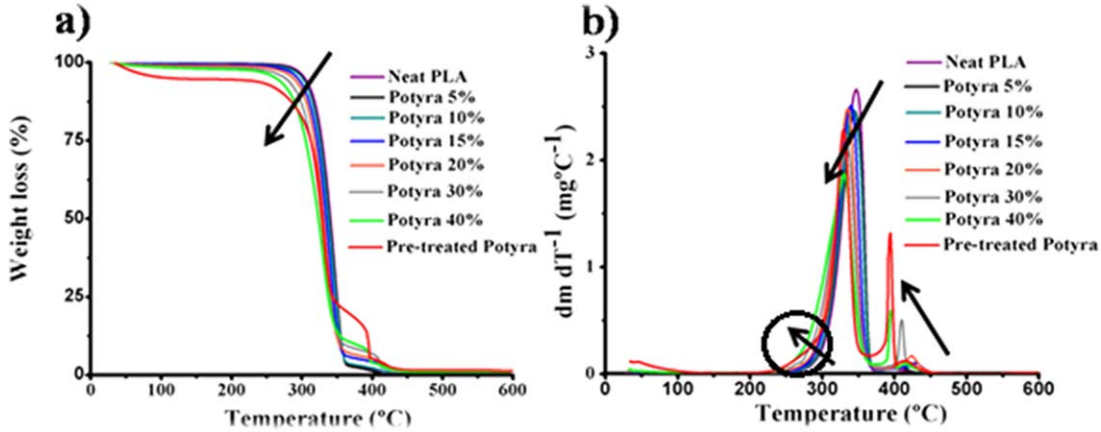

FIG. 1. (a) TG curves and (b) DTG curves of pretreated Potyra fibers, neat PLA and composites. [Color figure can be viewed at wileyonlinelibrary.com]

strength decrease [31]. PLA composites with cellulose extracted from newspaper also showed an impact strength reduction compared to the pure PLA matrix [30].

The onset temperatures (OOT) obtained from TGA curves decreased with the increasing fiber mass fraction, with the pure PLA showing the OOT of 322°C and the composite Potyra showing a 40% OOT reduction to 298°C (Table 1). According to Sena Neto [25], Potyra fibers show the initial degradation temperature of 264°C. The presence and increase of the fiber fraction initiates the degradation of the composite at lower temperatures due to the presence of hemicelluloses in the fibers [33]. The first peak of the derivative thermogravimetry (DTG) curve showed a shift to the left and a height reduction with the addition of PALF, anticipating the degradation events due the presence of hemicelluloses in the fiber (indicated by the black circle in Fig. 1) [33]. With the addition of PALF, a second peak appears at 380°C, corresponding to the degradation of lignin in the fibers [29, 34, 35].

DSC curves show the fibers acting as a nucleating agent, where the crystallinity fraction of the pure PLA was 15% and the crystallinity fraction of the 40% composite Potyra was 38% (Table 1).

The micrographs show no voids and contaminants for all formulations. For all composites, fiber bundles and individual fibers were observed. The quantity, length and diameter of the agglomerates were reduced with increasing Potyra PALF content. For Potyra 5% and Potyra 10% composites, regions with higher and lower reinforcement concentrations were present. The PALF addition in PLA caused an increase in the viscosity and therefore a shear stress increase. This increase in the shear stress causes a reduction of the agglomeration and leads to a better dispersion of the fibers throughout the matrix. There were voids or pull-outs arising from slippage of the fiber in relation to the matrix during cryogenic fracture for samples preparation (Fig. 2). The pull-outs are caused by two factors: first, there was no fiber-matrix interaction, and second, the fiber acted as a nucleating agent, leading to a volume contraction of the crystalline polymer so that the matrix moves away from the fiber. Conversely, anchor points are observed when approaching the region surrounding the fibers, indicating that the existence of interactions between the PLA and Potyra PALF (Fig. 2e). This anchoring leads to the charge transfer between the matrix and fiber, generating a mechanical reinforcement effect. Fiber treatment with NaOH aids in the appearance of these anchor points, because the cellulose hydroxyls become more exposed and the treatment dismantles the fiber bundles, increasing the area of interaction with the matrix. [13, 36, 37]. Starting at the concentration of 20 wt% Potyra PALF, an arrangement of fibers throughout the matrix was noticeable (Fig. 2f). This arrangement is referred to in the literature as a skin-core structure, and is due to fountain flow in injection molding [38–40].

Mean values and standard deviations of the fiber lengths, fiber diameters, fiber bundles lengths and fiber bundles diameters observed in the composites are shown in Table 2 and Fig. 3. The mean diameters of fiber units ranged from 2.5 to 3.6 μm, and average lengths ranged from 98 to 137 μm. The mean diameters of the fiber bundles ranged from 19 to 29 μm, and the average length ranged from 994 to 601 μm. For the variation of the average diameters and lengths of the fiber units with the volume concentration of the Potyra PALF in the composite, *P*-values smaller than 0.1 were not observed, as the linear regressions *R*-values were below 0.25. These *P*- and *R*-values indicate that there are no significant variances or linear correlation between the diameters and lengths of fiber units and fiber volumetric fraction in the PLA matrix. In all micrographs, no fiber units with sections that were reduced or damaged after the processing were observed, indicating that the fibers can withstand bending and twisting without breaking. Therefore, the average length (l) and diameters (d) of the fibers present in all compositions were obtained (Table 2).

 DOI 10.1002/pc

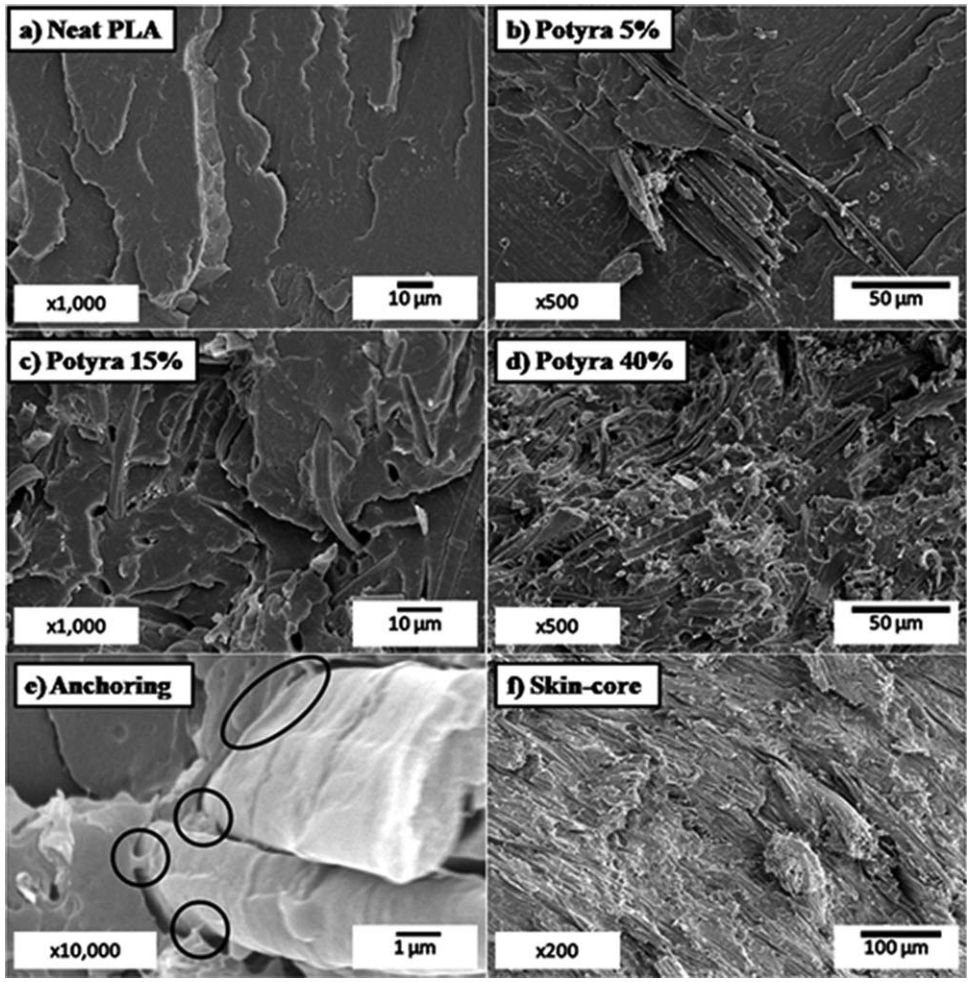

FIG. 2. SEM micrographs corresponding to neat PLA and composites.

For the average diameters and lengths of the fiber bundles, the *P*-values were less than 0.1. The *R*-values, in terms of volume fraction of Potyra PALF, were 0.48 and 0.74 for the fiber bundle length and diameter, respectively. These *P*- and *R*-values indicate significant variances and linear correlation between the diameters and lengths of fiber bundles with the fiber fraction present in the composite. The tensions during processing were sufficient to reduce the lengths and diameters of the fiber bundles. The breaking of the fiber bundles in extrusion and injection is induced by the following effects: bending caused by the interaction of fiber bundles with the shear flow melt, where the increase in the fiber length increases its chances of breaking [41]; the high viscosity caused by the fibers causing the increased shear stress on the bundles [38, 41, 42]; and the increase in the fraction of Potyra PALF led to the presence of a fiber-fiber interaction that aids in breaking the bundles.

The longitudinal modulus (E_{cl}) values were calculated using ξ equal to $2(l/d)$ for the l/d values given in Table 2. The fibers have l_f/d_f value equal to 36 (Table 2). For the bundles, the l_b/d_b value varied for each formulation, but was close to 36 (Table 2). For transverse Young's modulus (E_{ct}), ξ was considered to be equal to 2. Consequently, $E_{\mathbf{ctfiber}}$ is equal to $E_{\mathbf{ctbundle}}$.

The calculated Young's modulus with random fiber orientation ($E_{\mathbf{R\ fiber}}$) using the measured average fiber lengths and diameter varied between 2.8 and 10.9 GPa and between 2.8 and 10.7 GPa ($E_{\mathbf{R\ bundles}}$) when the measured average bundle lengths and diameters were used (Table 3). The theoretical values were higher than the

TABLE 2. Diameter of the fiber unit (d_f), length of the fiber unit (l_f), diameter of fiber bundles (d_b), and length of fiber bundles (l_b) for each composition.

Samples	d_f (µm)[a]	l_f (µm)[b]	l_f/d_f	d_b (µm)[a]	l_b (µm)[b]	l_b/d_b
Potyra 5%	$3.4^{(\pm 0.9)}$	$137^{(\pm 128)}$	—	$29^{(\pm 13)}$	$994^{(\pm 266)}$	35
Potyra 10%	$3.6^{(\pm 0.6)}$	$98^{(\pm 77)}$	—	$23^{(\pm 14)}$	$892^{(\pm 442)}$	38
Potyra 15%	$3.5^{(\pm 0.7)}$	$106^{(\pm 88)}$	—	$22^{(\pm 4)}$	$669^{(\pm 422)}$	31
Potyra 20%	$3.0^{(\pm 0.7)}$	$106^{(\pm 97)}$	—	$22^{(\pm 11)}$	$738^{(\pm 389)}$	33
Potyra 30%	$2.5^{(\pm 0.7)}$	$94^{(\pm 45)}$	—	$20^{(\pm 15)}$	$674^{(\pm 599)}$	33
Potyra 40%	$3.2^{(\pm 0.8)}$	$125^{(\pm 114)}$	—	$19^{(\pm 11)}$	$601^{(\pm 329)}$	32
Mean	$3.1^{(\pm 0.8)}$	$111^{(\pm 112)}$	36	—	—	—

[a]Measured by SEM micrographs.
[b]Measured by optical microscopy.

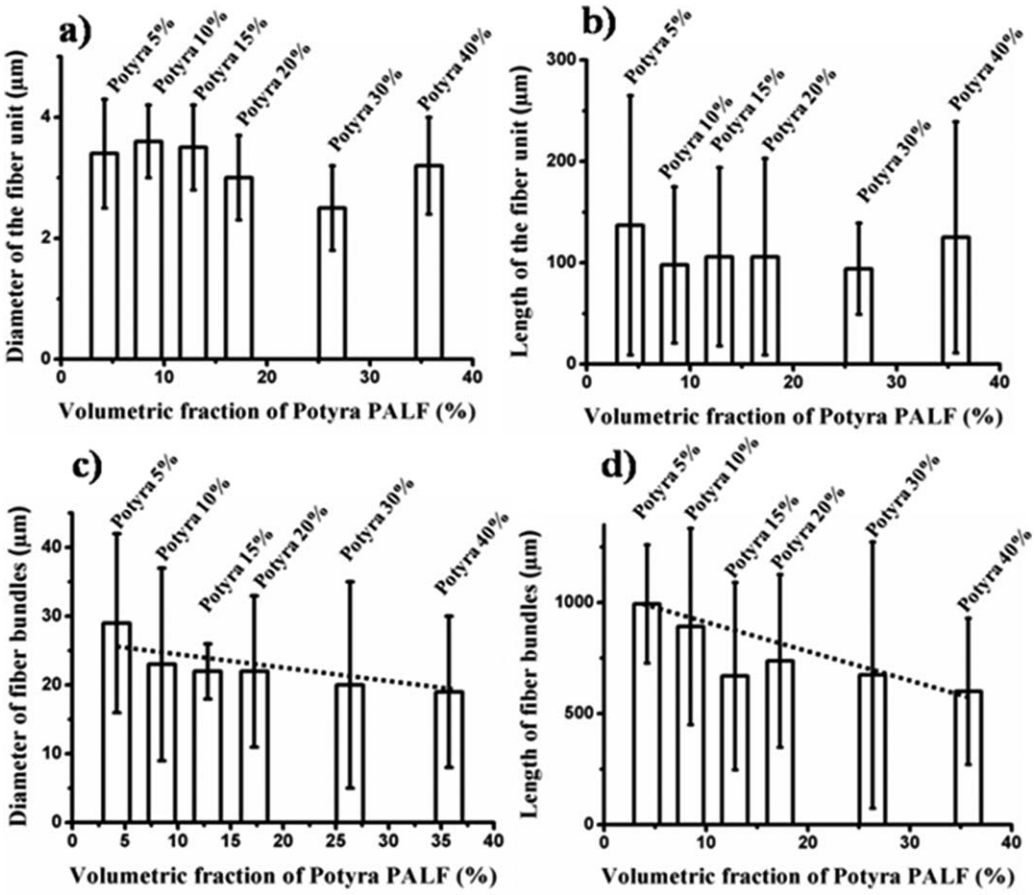

FIG. 3. Diameter and length of fibers and bundles.

Young's modulus values measured in the tensile test (2.1–3.5 GPa). This can be explained by the gap existing between the actual processing conditions and the ideal conditions of micromechanics theory: complete interfacial adhesion between matrix and reinforcement, complete distribution and dispersion of the reinforcements, and non-preferential orientation of reinforcements along the matrix. The measured Young's modulus values are closer to the theoretical Young's modulus values for the transverse orientation of the reinforcements. This may indicate that the fibers and fiber bundles are preferentially oriented in a direction transverse to the direction of injection flow and the direction of load axis in the tensile test (Fig. 2f).

Using the measured values of fiber diameters and fiber bundles, the critical length ($l_{\mathbf{R}}$) was calculated for each formulation according to Rosen's theory. Theoretical resistance was calculated for each composition from the $l_{\mathbf{R}}$ values. The fiber critical length value ($l_{\mathbf{R\ fibers}}$) was 29–71 μm (Table 4), and the fiber bundle critical length value ($l_{\mathbf{R\ bundles}}$) was 180–655 μm (Table 5). In both cases, there was a reduction in the critical length with increasing volume fraction of Potyra PALF. The lengths of the fibers and bundles were higher than the calculated $l_{\mathbf{R}}$. Theoretical tensile strength values ($\sigma_{\mathbf{t}}$) were between 44 and 149 MPa whereas the measured values ($\sigma_{\mathbf{m}}$) were between 54 and 70 MPa. The 5 wt% Potyra formulation

TABLE 3. Theoretical values of Young's modulus for each composition only with fibers oriented longitudinally ($E_{\text{cl fiber}}$) transversely ($E_{\text{ct fiber}}$), and randomly ($E_{\text{R fiber}}$).

Samples	$E_{\text{cl fiber}}$ (GPa)	$E_{\text{ct fiber}}$ (GPa)	$E_{\text{R fiber}}$ (GPa)	$E_{\text{cl bundles}}$(GPa)	$E_{\text{ct bundles}}$ (GPa)	$E_{\text{R bundles}}$ (GPa)	E_{measured} (GPa)
Potyra 5%	4.0	2.2	2.8	3.9	2.2	2.8	2.1 $^{(\pm 0.1)}$
Potyra 10%	6.1	2.4	3.8	6.1	2.4	3.8	2.4 $^{(\pm 0.0)}$
Potyra 15%	8.3	2.7	4.8	8.0	2.7	4.7	2.6 $^{(\pm 0.1)}$
Potyra 20%	10.6	3.0	5.9	10.4	3.0	5.8	2.9 $^{(\pm 0.0)}$
Potyra 30%	15.6	3.8	8.2	15.3	3.8	8.1	3.2 $^{(\pm 0.1)}$
Potyra 40%	21.2	4.8	10.9	20.6	4.8	10.7	3.5 $^{(\pm 0.1)}$

Theoretical values of Young's modulus for each composition only with fiber bundles oriented longitudinally ($E_{\mathbf{cl\ bundles}}$), transversely ($E_{\mathbf{ct\ bundles}}$), and randomly ($E_{\mathbf{R\ bundles}}$). Young's modulus value measured ($E_{\mathbf{measured}}$) for each composition according to tensile test.

 DOI 10.1002/pc

TABLE 4. Values of volume fraction ($Ø_f$), fiber critical length ($l_{R\ fibers}$) calculated by Rosen's theory, measured average fiber length ($l_{m\ fibers}$), theoretical tensile strength (σ_t) calculated from $l_{R\ fibers}$ obtained by Rosen's theory; and the measured tensile strength of the composite (σ_m).

Samples	$Ø_f$ (%)	$l_{R\ fibers}$ (μm)	$l_{m\ fibers}$ (μm)	l_m/l_R	σ_t (MPa)	σ_m (MPa)
Potyra 5%	4.21	71	**111**$^{(\pm 112)}$	1.6	45	54.5$^{(\pm 0.3)}$
Potyra 10%	8.49	56		2.0	57	56.6$^{(\pm 0.3)}$
Potyra 15%	12.84	48		2.3	71	59.5 $^{(\pm 0.4)}$
Potyra 20%	17.26	43		2.6	86	63.4$^{(\pm 0.2)}$
Potyra 30%	26.35	35		3.2	116	68.2$^{(\pm 1.1)}$
Potyra 40%	35.75	29		3.8	149	69.6$^{(\pm 1.5)}$

TABLE 5. Values of volume fraction ($Ø_f$), fiber bundle critical length ($l_{R\ bundles}$) calculated by Rosen's theory, measured average fiber bundle length ($l_{m\ bundles}$), theoretical tensile strength (σ_t) calculated from $l_{R\ bundles}$ obtained by Rosen's theory; and the measured tensile strength of the composite (σ_m).

Samples	$Ø_f$ (%)	$l_{R\ bundles}$ (μm)	$l_{m\ bundles}$ (μm)	I_m/I_R	σ_t (MPa)	σ_m (MPa)
Potyra 5%	4.21	655	994$^{(\pm 266)}$	1.5	44	54.5$^{(\pm 0.3)}$
Potyra 10%	8.49	426	892$^{(\pm 442)}$	2.1	58	56.6$^{(\pm 0.3)}$
Potyra 15%	12.84	340	669$^{(\pm 422)}$	2.0	69	59.5$^{(\pm 0.4)}$
Potyra 20%	17.26	308	738$^{(\pm 389)}$	2.4	84	63.4$^{(\pm 0.2)}$
Potyra 30%	26.35	232	674$^{(\pm 599)}$	2.9	115	68.2$^{(\pm 1.1)}$
Potyra 40%	35.75	180	601$^{(\pm 329)}$	3.3	147	69.6$^{(\pm 1.5)}$

showed theoretical values below the corresponding strengths measured by tensile tests. For Potyra 10%, σ_t was equal to σ_m. The formulations with higher fractions of Potyra PALF (from 15% to 40% PALF weight) showed measured tensile strength values that were lower than the calculated values. Rosen's theory considers the orientation of the fibers in the same axis direction as the load applied to calculate the critical length (I_R) [43]. As seen in the scanning electron microscopy (SEM) micrographs, the increase in the fraction of Potyra PALF causes the orientation of the fibers and bundles to become more transverse to the load application axis due to the injection flow (Fig. 2f). This preferentially transverse orientation of reinforcements causes the measured values of Young's modulus and tensile strength to be lower than those calculated by the theory. Conversely, there was an increase in the thermo-mechanical properties with increasing fraction of Potyra PALF in PLA composites as shown in this work.

CONCLUSIONS

The Potyra PALF acts as a nucleating agent, promoting faster crystallization of PLA and reaching the maximum crystallinity of 38% for the composite with 40 wt% Potyra PALF. SEM micrographs demonstrated that all composites showed well-distributed fiber bundles and individual fibers dispersed throughout the matrix. The skin-core structure was observed for compositions with a high PALF fraction, indicating the orientation of the fibers with the injection flow. There were no changes in the morphological dimensions of the fiber units, indicating that they support the stresses during the extrusion and injection processes. The aspect ratio for the fiber units was 36. Conversely, fiber bundles are susceptible to stress during processing. The bundle diameter decreased from 29 to 19 μm, and the bundle length decreased from 994 to 601 μm. The aspect ratio of the fiber bundles remained between 31 and 38. The measured Young's modulus and tensile strength values of the composites were lower than the theoretical values obtained by micromechanics theory, indicating that the fibers were oriented by injection flow and suggesting that there was no overall reinforcement-matrix adhesion. Conversely, there were also adhesion points between the PLA and fiber that provided the load transfer between the matrix and the reinforcement. Young's modulus increased 79% with the addition of Potyra PALF. The tensile strength also increased, reaching 70 MPa for Potyra 40%. The addition of fibers also led to a 66% increase in the impact strength for the Potyra 40% composite. The HDT of the composite also increased, reaching a 10% increase for Potyra 40%. This study showed that the pre-treated Potyra PALF fibers show potential for use as reinforcement in green composites.

REFERENCES

1. E. McLaughlin and R. Tait, *J. Mater. Sci.*, **15**, 89 (1980).
2. L. Averous and N. Boquillon, *Carbohydr. Polym.*, **56**, 111 (2004).
3. M.A. Martins, P.K. Kiyohara, and I. Joekes, *J. Appl. Polym. Sci.*, **94**, 2333 (2004).
4. K. Sao, B. Samantaray, and S. Bhattacherjee, *J. Appl. Polym. Sci.*, **52**, 1687 (1994).
5. S.V. Joshi, L. Drzal, A. Mohanty, and S. Arora, *Compos. Part A: Appl. Sci. Manuf.*, **35**, 371 (2004).
6. P. Mukherjee and K. Satyanarayana, *J. Mater. Sci.*, **19**, 3925 (1984).
7. S. Luo and A. Netravali, *J. Mater. Sci.*, **34**, 3709 (1999).
8. A.L. Leao, J. C. Caraschi, and I. Tan, "Curaua fiber - A tropical natural fibers from Amazon potential and applications in composites." *Natural Polymers and Agrofibers*

Bases Composites Embrapa Instrumentacao, Sao Carlos, Brazil 257–272 (2000).
9. A. Mohanty, P. Tripathy, M. Misra, S. Parija, and S. Sahoo, *J. Appl. Polym. Sci.*, **77**, 3035 (2000).
10. N. Reddy and Y. Yang, *Trends Biotechnol.*, **23**, 22 (2005).
11. A. Leão, I. Machado, S. De Souza and L. Soriano, "Production of curaua (Ananas Erectifolius LB SMITH) fibers for industrial applications: characterization and micropropagation," *Acta Hortic* 822, 227–238 (2009). doi: 10.17660/Acta Hortic.
12. G. Marques, A. Gutierrez, and J.C. del Rio, *J. Agric. Food Chem.*, **55**, 1327 (2007).
13. M.S. Huda, L.T. Drzal, A.K. Mohanty, and M. Misra, *Compos. Interfaces*, **15**, 169 (2008).
14. N. Lopattananon, Y. Payae, and M. Seadan, *J. Appl. Polym. Sci.*, **110**, 433 (2008).
15. J. R. S. Cabral, M. da S. Castellen, F. Souza, A. de Matos, and F. FEREIRA, Banco ativo de germoplasma de abacaxi. Embrapa Mandioca e Fruticultura, Cruz das Almas, Brazil. Documentos, 146 (2004). https://www.infoteca.cnptia.embrapa.br/bitstream/doc/653901/1/documento146.pdf.
16. G. M. Bohlmann, Handbook of Biodegradable Polymers, Rapra Technology Ltd, Shawbury, UK 183–212 (2005).
17. J.S. Dugan, *Int. Nonwovens J.*, **10**, 29 (2001).
18. D. Garlotta, *J. Polym. Environ.*, **9**, 63 (2001).
19. D.E. Henton, P. Gruber, J. Lunt, and J. Randall, *Nat. Fibers, Biopolym., Biocompos.*, **16**, 527 (2005).
20. S. Kalia and L. Avérous, Biopolymers: Biomedical and Environmental Applications, John Wiley & Sons, Salem, USA (2011).
21. E. Hassan, Y. Wei, H. Jiao, and Y.M. Hou, *Int. J. Eng. Sci. Technol.*, **1**, 4429 (2012).
22. S.-H. Lee, and S. Wang, *Compos. Part A: Appl. Sci. Manuf.*, **37**, 80 (2006).
23. Y. Li and X. Susan Sun, *J. Appl. Polym. Sci.*, **121**, 589 (2011).
24. P. Jandas, S. Mohanty, and S. Nayak, *J. Polym. Environ.*, **20**, 583 (2012).
25. A.R.S. Neto, M.A. Araujo, R.M. Barboza, A.S. Fonseca, G.H. Tonoli, F.V. Souza, L.H. Mattoso, and J.M. Marconcini, *Ind. Crops Prod.*, **64**, 68 (2015).
26. B.D. Agarwal, L.J. Broutman, and K. Chandrashekhara, Analysis and performance of fiber composites. John Wiley & Sons, New York, USA (2006).
27. K. Chawla, Composite Materials: Science and Engineering, Springer, New York (1998).
28. B. W. Rosen Mechanics of composite strengthening. Fiber Composite Materials. American Society of Metals, Metals Park, Ohio 37 (1965).
29. M.A.M. de Araujo, S. Neto, E. Hage, L.H.C. Mattoso, and J.M. Marconcini, *Polym. Compos.*, **36**, 1520–1530 (2015).
30. M.S. Huda, L.T. Drzal, A.K. Mohanty, and M. Misra, *Compos. Sci. Technol.*, **66**, 1813 (2006).
31. B. Bax and J. Müssig, *Compos. Sci. Technol.*, **68**, 1601 (2008).
32. M. Huda, L. Drzal, M. Misra, and A. Mohanty, *J. Appl. Polym. Sci.*, **102**, 4856 (2006).
33. M. Rosa, E. Medeiros, J. Malmonge, K. Gregorski, D. Wood, L. Mattoso, G. Glenn, W. Orts, and S. Imam, *Carbohydr. Polym.*, **81**, 83 (2010).
34. H.J. Kim and Y.G. Eom, *J. Korean Wood Sci. Technol.*, **29**, 9 (2001).
35. E. Corradini, E. Teixeira, P. Paladin, J. Agnelli, O.R. Silva, and L.H. Mattoso, *J. Thermal Anal. Calorimetry*, **97**, 415 (2009).
36. M.S. Huda, L.T. Drzal, A.K. Mohanty, and M. Misra, *Compos. Sci. Technol.*, **68**, 424 (2008).
37. M.A. Sawpan, K.L. Pickering, and A. Fernyhough, *Compos. Part A: Appl. Sci. Manuf.*, **42**, 1189 (2011).
38. P. Mallick and S. Newman, *Composite Materials Technology*, Hanser, Munich (1990).
39. S.G. Advani, Flow and Rheology in Polymer Composites Manufacturing, Elsevier Science, New York, USA, **10** (1994).
40. Z. Tadmor, *J. Appl. Polym. Sci.*, **18**, 1753 (1974).
41. T. Papthanasiou and D. C. Guell (Ed.), FFlow-Induced Alignment in Composite Materials, Elsevier, Cambridge, England (1997).
42. R.F. Landel and L.E. Nielsen, Mechanical Properties of Polymers and Composites, CRC Press, New York, USA (1993).
43. Y. Wyser, Y. Leterrier, and J.A. Månson, *J. Appl. Polym. Sci.*, **78**, 910 (2000).